

Electronic supplementary information (ESI)

Phenyl-Triazine Oligomers for Light-Driven Hydrogen Evolution

K. Schwinghammer, ‡^a S. Hug, ‡^a M. B. Mesch,^b J. Senker,^b and B. V. Lotsch^{a*}

* Author to whom correspondence should be addressed. Tel: +49-711-689-1610, Fax: +49-711-689-1612. E-mail: b.lotsch@fkf.mpg.de

^a Max Planck Institute for Solid State Research, 70569 Stuttgart, Germany. Department of Chemistry, University of Munich, LMU, 81377 Munich, Germany. Nanosystems Initiative Munich (NIM) and Center for NanoScience (CeNS), 80799 Munich, Germany.

^b Inorganic Chemistry III, University of Bayreuth, 95447 Bayreuth, Germany.

‡ These authors contributed equally

Table of Content

Experimental Section.....	S2
Characterization of the PTO _{organic phase}	S8
XRD Characterization.....	S9
Elemental Analysis and ICP.....	S9
XPS Measurements.....	S10
MALDI-TOF Measurements and IR Analysis.....	S11
Ar-Physisorption Measurements.....	S19
NMR Measurements.....	S21
Photocatalytic Experiments.....	S22
TEM Characterization.....	S30

Experimental Section

Methods

Argon adsorption/desorption measurements were performed at 87 K with an Autosorb-iQ surface analyzer (Quantachrome Instruments, USA). Samples were outgassed in vacuum at 120 °C for 6-12 h to remove all guests. For BET calculations pressure ranges of the Ar isotherms were chosen with the help of the BET Assistant in the ASiQwin software. In accordance with the ISO recommendations multipoint BET tags equal or below the maximum in $V \cdot (1 - P/P_0)$ were chosen.

Infrared (IR) spectroscopy measurements were carried out on a Perkin Elmer Spektrum BX II (Perkin Elmer, USA) with an attenuated total reflectance unit.

Powder X-ray diffraction (PXRD) was measured on a BRUKER D8 Avance (Bruker AXS, USA) in Bragg-Brentano geometry with a Cu-K α_1 -radiation ($\lambda = 1.54051$ Å).

Elemental analysis (EA) was carried out with an Elementarvario EL (Elementar Analysensysteme, Germany).

Energy dispersive X-ray spectroscopy (EDX) was carried out on a JEOL JSM-6500F electron microscope (JEOL, Japan) with a field emission source equipped with an EDX detector (model 7418, Oxford Instruments, UK) and a Tescan Vega TS 5130MM electron microscope equipped with a Si/Li EDX detector (Oxford Instruments, UK).

Inductively coupled plasma atomic emission spectroscopy (ICP-AES) was carried with a pressure digestion system by Berghof, a plasma created on a Vista Pro ICP-AES spectrometer, an Echelle-Polychromator by Fa. Varian Darmstadt and a photomultiplier.

^{13}C magic angle spinning (MAS) solid-state nuclear magnetic resonance (ssNMR) spectra were recorded at ambient temperature on a BRUKER DSX Avance 500 FT and a BRUKER AvanceIII HD 400 NMR spectrometer (Bruker Biospin, Germany) with external magnetic fields of 11.8 T and 9.4 T, respectively. The operating frequencies are 500.1 MHz and 125.7 MHz and 400.1 MHz and 100.6 MHz for ^1H and ^{13}C , respectively, and the spectra were referenced relative to TMS. The samples were contained in 4 or 3.2 mm ZrO_2 rotors and mounted in standard triple resonance BRUKER MAS probes. The spinning speed was set to 10 kHz or 20 kHz (for the photocatalyst after photocatalysis, CTF-1 and quantitative ^{13}C measurements). During acquisition of the spectra ^1H decoupling (approx. 70 kHz RF field) was applied using a SPINAL64 sequence.

For $^1\text{H}/^{13}\text{C}$ ramp-amplitude (RAMP) cross-polarization (CP) MAS spectra a contact time of 5 ms and a 90° pulse length of 2.50 μs on ^1H was set. The quantitative ^{13}C measurements were recorded using a single pulse (SP) experiment. The recycle delay was varied between 60 and 6000 s for PTO-300-10, to get an idea about the T_1 . For the final measurements a recycle delay of 6000 s was used and 64 scans were executed. The background signal was recorded using a

recycle delay of 0.5 s to make sure that only the background signal is relaxed and gives a signal. This signal was subtracted from the spectrum.

$^1\text{H}/^{15}\text{N}$ CP MAS ssNMR spectra were measured at ambient temperature on a BRUKER AvanceIII HD 400 NMR (PTO-300-1 und -10) and a BRUKER AvanceII 300 (CTF-1) NMR spectrometer with external magnetic fields of 9.4 T and 7.1 T, respectively. The operating frequencies are 400.1 MHz and 40.6 MHz and 300.1 MHz and 30.4 MHz for ^1H and ^{15}N , respectively.

The samples were contained in 4 or 7 mm ZrO_2 rotors which were mounted in standard double or triple resonance BRUKER MAS probes. The spinning speed was set to 10 or 5 kHz and the chemical shifts were referenced relative to nitromethane. During acquisition of the spectra ^1H decoupling (approx. 70 kHz RF field) was applied using a SPINAL64 sequence.

The spectra were recorded using a RAMP CP pulse on ^1H with a nutation frequency ν_{nut} of 40 kHz and 45 kHz on ^{15}N , respectively. During a contact time of 5 ms the ^1H RF field was linearly varied about 50%. The recycle delay was set to 2 s and 1.5 s. About 120000 and 40000 transients were accumulated for the CP experiments, respectively.

For X-ray photoelectron spectroscopy (XPS), samples were pressed onto indium foil and the spectra were collected on an Axis Ultra (KRATOS Analytical, Manchester) X-ray photoelectron spectrometer with charge neutralization. The spectra were processed using the software OriginPro 8.5.1 and fitted with the Gaussian function. The spectra were referenced to the adventitious carbon 1s peak at 284.600 eV. Binding energies were compared with the NIST Standard Reference Database 30 (Version 4.1) unless otherwise specified.

Matrix-assisted laser deposition/ionization-time of light (MALDI-TOF) was performed on a Shimadzu Axima Resonance mass spectrometer. Calibration was carried out using neat fullerene and using CsI ground with *trans*-2-[3-(4-*tert*-butylphenyl)-2-methyl-2-propenylidene] malononitrile as the matrix. Each sample was ground with dithranol ($m/z = 227$) as the matrix and deposited on a steel sample holder. The spectra were collected in raster mode and the laser power was progressively increased until a suitable signal-to-noise ratio was achieved. The presented spectra are averaged from 100 profiles.

Optical diffuse reflectance spectra of the solids were collected at room temperature with a UV-Vis-NIR diffuse reflectance spectrometer Cary 5000 (Agilent Technologies, USA) at a photometric range of 250-800 nm. Powders were prepared in a sample carrier with a quartz glass window at the edge of the integrating sphere with BaSO_4 as the optical standard. Kubelka-Munk spectra were calculated from the reflectance data.

TEM was performed with a Philips CM 30 ST microscope (LaB_6 cathode, 300 kV, CS = 1.15 mm). Images were recorded with a CCD camera (Gatan) and Digital Micrograph 3.6.1 (Gatan) was used as evaluation software.

Hydrogen evolution experiments in UV and simulated sunlight were carried out in a continuously cooled 230 mL quartz glass reactor (see Fig. S1) with a PTFE septum under argon

atmosphere. The catalyst (10 mg) was suspended in a 0.5 M pH7 phosphate buffer solution (9 mL), triethanolamine (TEoA) was used as the sacrificial electron donor (1 mL), and H_2PtCl_6 (6 μL of 8 wt% in H_2O , ≈ 2.2 wt% Pt, Fig. S25†) was added as precursor for the *in situ* formation of the Pt co-catalyst while stirring. Buffered water conditions lead to higher activities and a more stable hydrogen evolution rate than using non-buffered water (Fig. S18†). The flask was evacuated and purged with argon to remove any dissolved gases in the suspension. Samples were simultaneously top-illuminated (top surface = 15.5 cm^2) at a distance of 22 cm with a 300 W xenon lamp with a water filter and dichroic mirror (Newport Oriel) blocking most of the wavelengths $< 420\text{ nm}$ for simulated sunlight (spectral profile see Fig. S2) and $< 250\text{ nm}$ for UV-Vis measurements, which amounts to a light intensity of about 380 mW cm^{-2} for the simulated sunlight and 510 mW cm^{-2} for the $\geq 250\text{ nm}$ measurements on the surface of the sample.

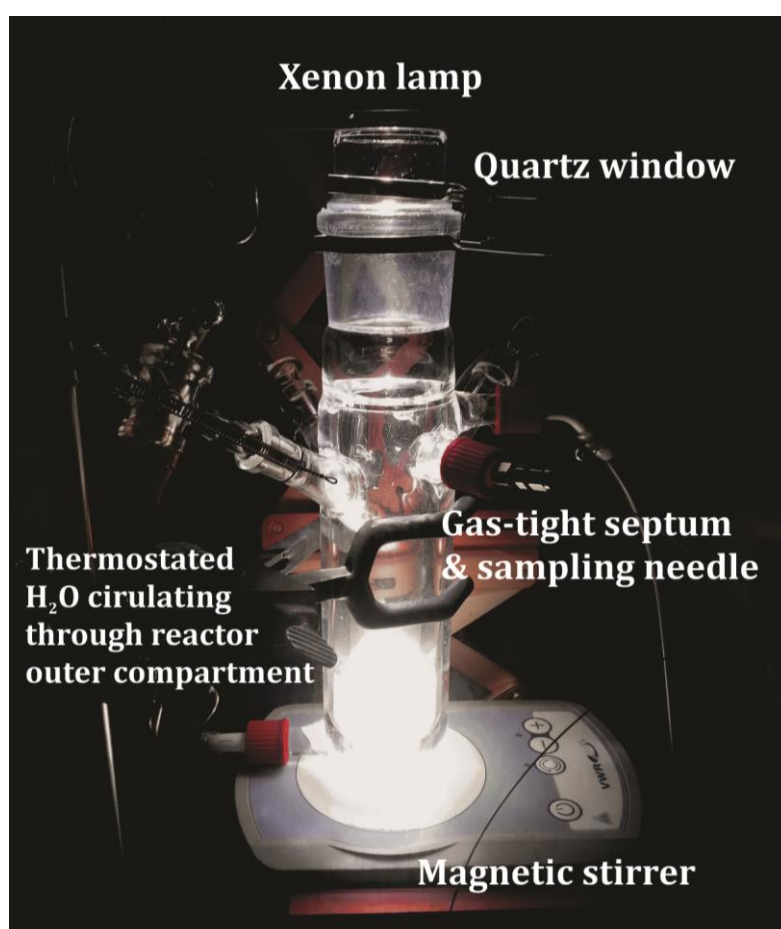


Fig. S1 Reactor set-up used for evaluating photocatalysts for hydrogen evolution.

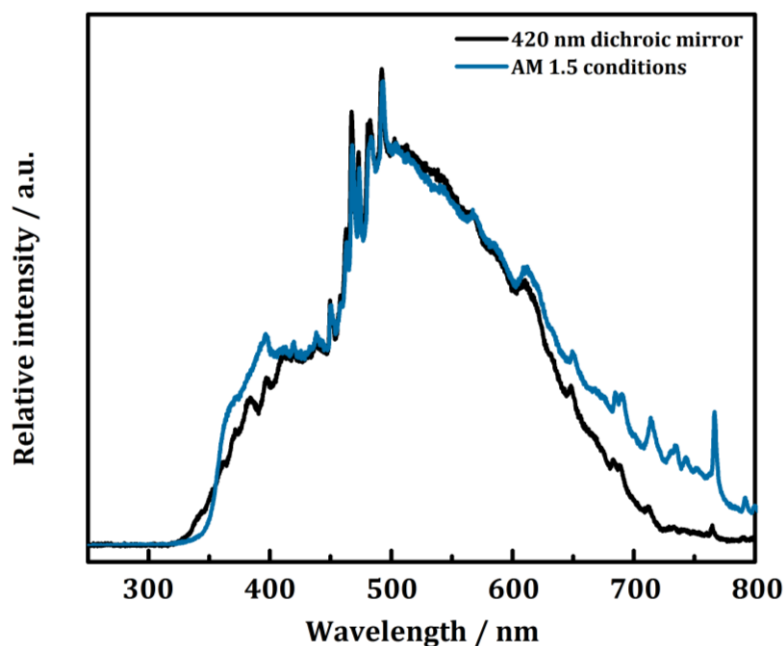


Fig. S2 Light intensity profile of the Xe lamp using the ≥ 420 nm dichroic mirror (simulated sunlight) compared to the AM 1.5 filter (filter and mirror purchased from Newport Oriel). Spectra were recorded with an Ocean Optics USB4000-XR1-ES spectrometer.

The headspace of the reactor was periodically sampled with an online injection system and the gas components were quantified by gas chromatography (thermal conductivity detector, argon as carrier gas). A high hydrophobicity of the CTF-1 and PTO samples was noticed at the beginning which was reduced during the photocatalytic experiment due to a better dispersion of the photocatalyst. Interestingly, the hydrogen evolution rates of the PTO-300s (> 1 eq ZnCl_2) illuminated with simulated sunlight were just slightly lower than for the samples illuminated with ≥ 250 nm. Apparent quantum efficiency calculations were estimated according to $\text{QE}\% = (2 \times H) / P \times 100 / 1$, where H = number of evolved hydrogen molecules and P = incident number of photons on the sample. The incident light was measured with a thermopile power meter with a constant efficiency response across the visible spectrum. Wavelength specific hydrogen evolution experiments were carried out in a 30 mL glass vial also in an argon atmosphere with PTFE/Teflon septa. The samples were top-illuminated for four hours with a full spectrum mirror (≥ 250 nm) and additional 40 nm FWHM light filters (400, 450, 500, 550 or 600 nm) (Thor labs). The irradiation area was 3.6 cm^2 . The hydrogen evolution rates were normalized with respect to an irradiation intensity on the sample surface of 14 mW cm^{-2} . For the internal comparison with other organic photocatalysts (Melon, PTI nanosheets and TFPT-COF), reported conditions for these materials were chosen which means using water instead of the buffered solution.

Four different PTO-300 samples were also tested under AM 1.5 conditions (100 mW cm^{-2}) which is shown in Figure S20.

Materials

All reactions were carried out under an argon atmosphere in flame-dried glassware. 1,4-Dicyanobenzene (98%), DMF (99.8%) and 1,5-*bis*(diphenylphosphino)pentane (97%) were obtained from Acros Organics. Anhydrous zinc chloride (99.995%, 25 mg product sealed in an ampule), 4-bromobenzonitrile (99%) and Pd(PPh₃)₄ (99%) were purchased from Sigma-Aldrich. Triflic acid and zinc cyanide (98%) were received from Alfa Aesar (98%) and used without further purifications.

Synthesis of photoactive phenyl-triazine oligomers (PTO). In a typical CTF synthesis^{S1} a Duran ampule (1.5 x 12 cm) was charged with finely ground 1,4-dicyanobenzene (500 mg, 3.90 mmol) and ZnCl₂ (1-15 equivalents, see Table 1) within a glove box. The ampule was flame sealed under vacuum and was subjected in a tube oven to temperatures between 300-350 °C for 168-96 h (see Table 1). After cooling to ambient temperature, the ampule was opened and its content ground thoroughly. An inhomogeneous temperature zone in addition to a high zinc chloride content yielded colorless, fiber-like crystals (which are not discussed here). The crude product was stirred in H₂O (75 mL) for 1 h, filtered, and washed with 1 M HCl (2 × 75 mL). The mixture was then stirred at 90 °C in 1 M HCl (75 mL) overnight, filtered, and subsequently washed with 1 M HCl (3 × 75 mL), H₂O (12 × 75 mL), THF (2 × 75 mL), and dichloromethane (1 × 75 mL). Finally, the powder was dried overnight in a desiccator.

Synthesis of CTF-1.^{S1} Similar to the synthesis described above, CTF-1 was obtained starting with 1,4-dicyanobenzene (500 mg, 3.90 mmol) under ZnCl₂ (1 equivalent) conditions at a reaction temperature of 400 °C for 46 hours.

Synthesis of 2,4,6-*tris*(*p*-bromophenyl)-1,3,5-triazine. This compound was prepared as per a modified literature procedure.^{S2} To a 15 ml Schlenk tube under argon, triflic acid (4.0 ml, 6.7 g, 44.6 mmol) was added and cooled to 0 °C. To this, 4-bromobenzonitrile (1.5 g, 8.2 mmol) was added in portions and the solution was continued to stir for an hour at 0 °C and then 16 hours at room temperature. The workup was done by pouring the reaction mixture in 100 mL ice cold water and neutralizing the resulting suspension with 25% ammonia solution. The precipitate was filtered off, washed with water (2 x 10 mL), acetone (3 x 5 mL) and dried in vacuum to afford the title compound as off-white solid (1.4 g, 94%). ¹H NMR (CDCl₃, 300 MHz): δ ppm 8.59 (d, *J* = 8.4 Hz, 6H), 7.72 (d, *J* = 8.4 Hz, 6H). ¹³C NMR (CDCl₃, 75 MHz): δ ppm 171.37, 135.07, 132.10, 130.55, 127.88.

Synthesis of 2,4,6-*tris*(*p*-cyanophenyl)-1,3,5-triazine (Trimer). In a microwave vial charged with DMF (10.0 mL), a stream of argon was bubbled for 30 min. To this was then added 2,4,6-*tris*(*p*-bromophenyl)-1,3,5-triazine (200 mg, 0.37 mmol), Zn(CN)₂ (67 mg, 0.57 mmol), Pd(PPh₃)₄ (25 mg, 0.022 mmol), and 1,5-*bis*(diphenylphosphino)pentane (10 mg, 0.022 mmol). The vial was sealed and the contents were heated in a microwave for 20 min at 150 °C. The resulting suspension was poured into water (100 mL) and then filtered, washed with water

(20 mL x 2), saturated sodium bicarbonate solution (10 mL x 2) and methanol (20 mL x 2) to obtain the crude product that was purified by flash chromatography (CHCl_3) to obtain 2,4,6-tris(*p*-cyanophenyl)-1,3,5-triazine (Trimer) (120 mg, 85%) as colorless solid. ^1H NMR 300 MHz ($\text{C}_2\text{D}_2\text{Cl}_4$; 70 °C): δ 8.87 (d, J = 8.3 Hz, 6H), 7.93 (d, J = 8.3 Hz, 6H). ^{13}C NMR 75 MHz ($\text{C}_2\text{D}_2\text{Cl}_4$; 70 °C): δ 170.90, 139.14, 132.46, 129.39, 118.09, 116.30. MS (MALDI): m/z : 384.4.

Synthesis of Melon.^{S3} A porcelain crucible was loaded with dicyandiamide and heated in a muffle furnace at 600 °C for 4 hours. The synthesis yielded a yellow colored powder.

Synthesis of 16% 4-AP doped amorphous PTI.^{S4} Dicyandiamide (0.50 g, 5.95 mmol), an eutectic mixture of lithium chloride (59.2 mol%) and potassium chloride (40.8 mol%) and 4-AP (72 mg, 16 % carbon-doping) as doping agent were ground and transferred in open porcelain crucibles, which were heated in a Argon purged horizontal tube furnace at 12 °C min⁻¹ to 550 °C for 6 hours. After grinding the sample, the heating procedure was repeated to gain a homogenous polymerized product. The syntheses yielded in a dark orange colored product which is in accordance with the literature.^{S4}

Synthesis of TFPT-COF and PTI-nanosheets according to the literature.^{S5,6}

Characterization of PTO_{organic phase}

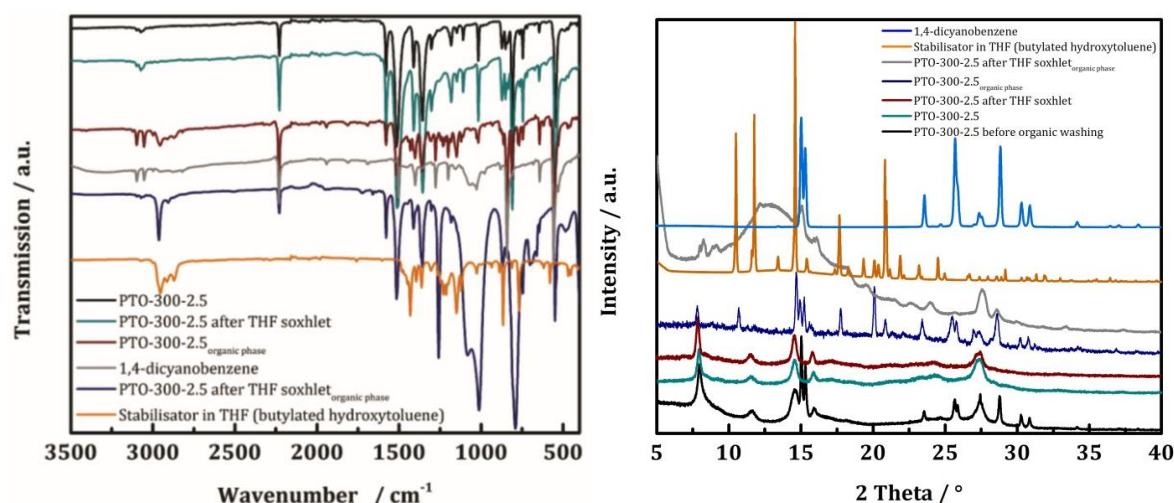


Fig. S3 Exemplary IR spectra (left) and PXRDs (right) of the obtained organic phase after washing PTO-300-2.5 using THF and DCM (PTO-300-2.5_{organic phase}) compared to pristine PTO-300-2.5, after further THF Soxhlet extraction, and of its organic phase from Soxhlet extraction. The IR spectra of the starting material 1,4-dicyanobenzene and of the THF-stabilizer butylated hydroxyl toluene is added for clarity. The first organic phase contains unreacted starting material and most likely smaller oligomers. The organic phase obtained by Soxhlet extraction includes also stabilizer impurities.

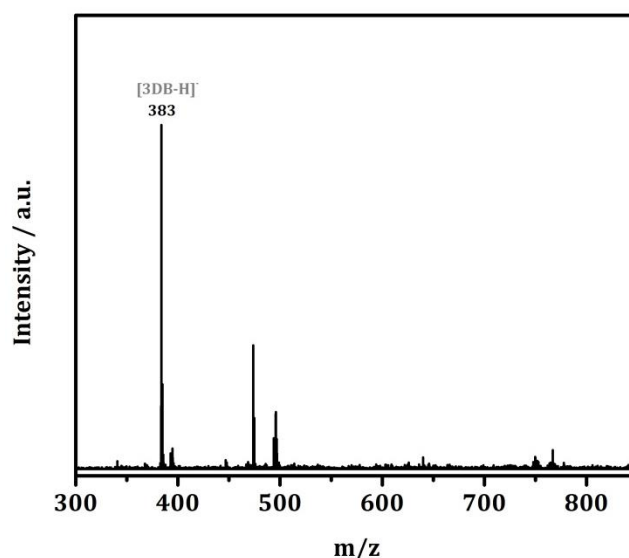


Fig. S4 MALDI-TOF spectrum (negative mode) of PTO-300-15_{organic phase} showing a trimer fragment. No signals were observed in the mass ranges below 300 and above 850.

XRD Characterization

Table S1 Shift of the layer stacking from PTO-300-1 to PTO-300-15 compared to CTF-1.

Sample	2 Theta / °	Layer distance [Å]
CTF-1 ^{S1}	26.2	3.40
PTO-300-1	26.8	3.32
PTO-300-2.5	27.3	3.26
PTO-300-5	27.3	3.26
PTO-300-10	27.3	3.26
PTO-300-15	27.3	3.26

Elemental Analysis and ICP

Table S2 Elemental analysis and BET surface areas of the presented PTOs compared to CTF-1 and calculated theoretical values of the elemental composition of 1,4-dicyanobenzene and the trimer.

Sample	N [wt%]	C [wt%]	H [wt%]	Zn [wt%] ^d	wt.% C/N	BET SA ^a [m ² g ⁻¹]
Calculated	21.86	74.99	3.15	0	3.43	-
1,4-dicyanobenzene and trimer	21.86	74.99	3.15	0	3.43	-
CTF-1 according to Kuhn <i>et al.</i> ^{S1}	19.3	72.8	3.2	-	3.77	791
CTF-1 according to Ren <i>et al.</i> ^{b S7}	20.71	74.49	3.03	-	3.60	2
CTF-1 according to Ren <i>et al.</i> ^{c S7}	22.58	72.93	3.32	-	3.23	4
PTO-300-1	21.61	74.30	3.29	0.03	3.44	116
PTO-300-2.5	21.38	73.53	3.23	0.02	3.44	12
PTO-300-5	21.57	74.25	3.28	0.04	3.44	19
PTO-300-10	21.69	74.45	3.32	0.11	3.43	13
PTO-300-15	20.99	72.75	3.48	0.03	3.47	21
PTO-350-1	21.13	73.59	3.34	0.01	3.48	10
PTO-350-10	20.39	72.93	3.15	0.01	3.58	6
CTF-1 as synthesized	18.60	70.20	3.30	0.21	3.77	610

^aFrom argon physisorption measurements (Figure S21-22). ^bTFMS catalysed synthesis and further heating step at 400 °C for 40 h. ^cTFMS catalysed and microwave-assisted synthesis. ^dMeasured by ICP.

XPS Measurements

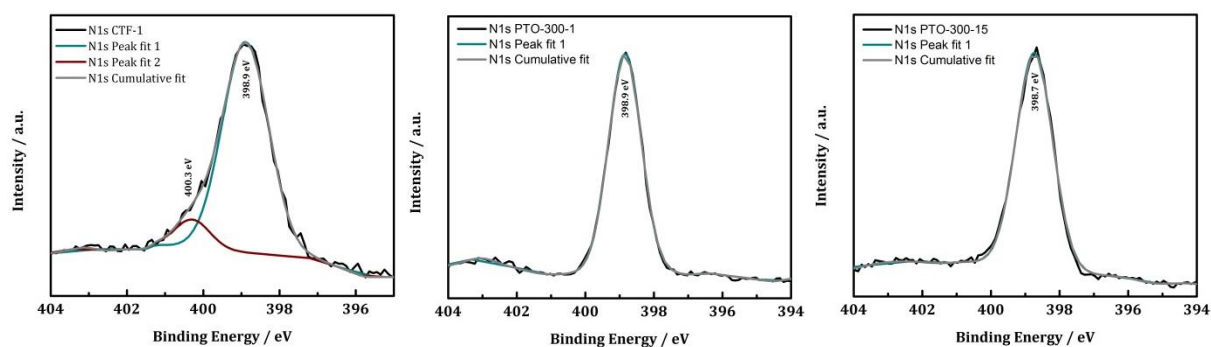


Fig. S5 N1s XPS spectra with applied peak and cumulative fits of CTF-1 (left), PTO-300-1 (middle) and PTO-300-15 (right).

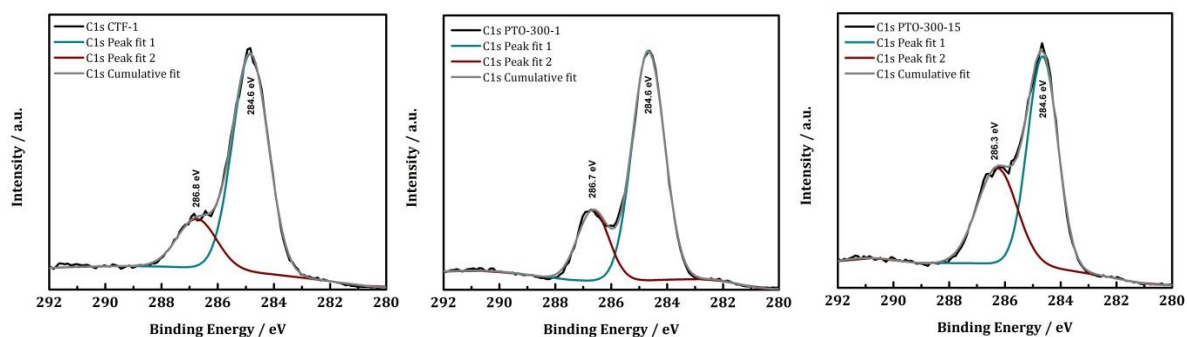


Fig. S6 C1s XPS spectra with applied peak and cumulative fits of CTF-1 (left), PTO-300-1 (middle) and PTO-300-15 (right).

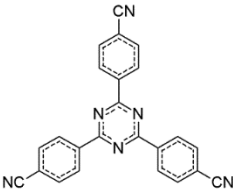
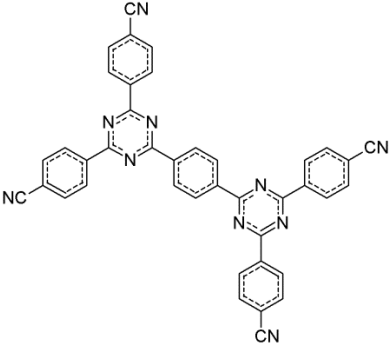
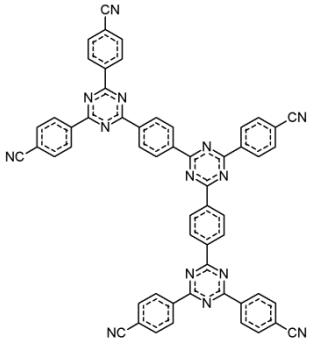
MALDI-TOF Measurements and IR Analysis

Table S3 Summarized mass peaks observed in the MALDI-TOF spectra of PTO-300-1 and PTO-300-15.

PTO-300-1	PTO-300-15	Connectivity
128	128	monomer
256		dimer
384	384	trimer
641	641	pentamer (chain, dendrimer)
897	897	heptamer (chain, dendrimer)
1153	1153	nonamer (chain, dendrimer)
-	1409	endecamer (chain, dendrimer)
1499	1551	dodecamer (chain or ring) without 1CN (PTO-300-1) or with 1N (PTO- 300-15)
2049	-	16mer
2178	-	17mer (chain, dendrimer)
2306	-	18mer
2434	-	19mer (chain, dendrimer or ring)
2563	-	20mer
2690	-	21mer (chain, dendrimer)
2819	-	22mer
2947	-	23mer (chain)

Dendrimers: $(3 + 2n; n = 0, 1, 2, 3,...)$ multiples of 1,4-dicyanobenzene mass ($m/z = 128.1$)

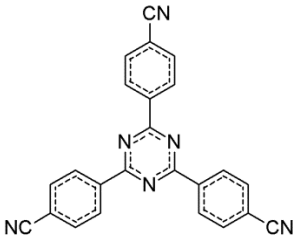
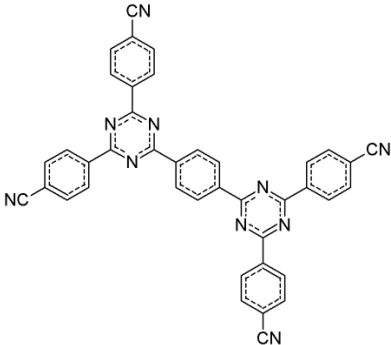
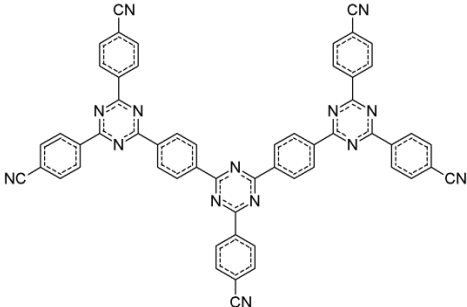
Table S4 Observed dendrimeric oligomers of CTF-1 and the specific nitrile-to-triazine ratio.

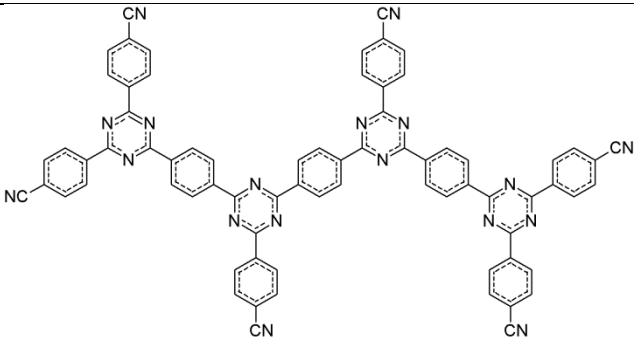
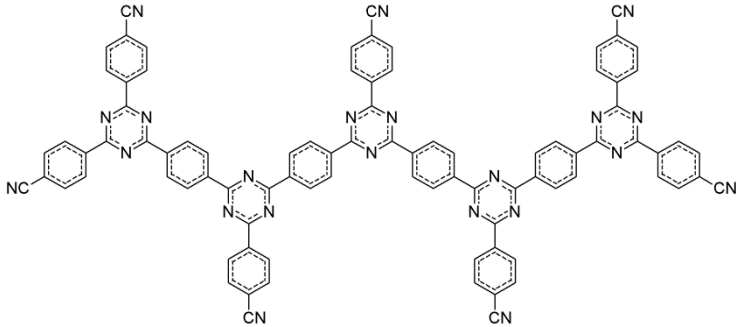
Chain Fragments	n	$(3+2n)$	m/z	Number of $C\equiv N$ / Number of $C=N$ bonds
	0	3	384.4	$3 / 6 \cdot 1 = 0.50$
	1	5	640.7	$4 / 6 \cdot 2 = 0.33$
	2	7	896.9	$5 / 6 \cdot 3 = 0.28$

	3	9	1153.2	$6 / 6 \cdot 4 = 0.25$
	6	15	1922.0	$9 / 6 \cdot 7 = 0.21$
	8	19	2434.5	$11 / 6 \cdot 9 = 0.20$

Chain Fragments: $(3 + 2n; n = 0, 1, 2, 3,...)$ multiples of 1,4-dicyanobenzene mass ($m/z = 128.1$)

Table S5 Linear chain fragments (of CTF-1) observable in the mass spectra for the PTO samples and the specific nitrile-to-triazine ratio.

Chain Fragments	n	$(3+2n)$	m/z	Number of $C\equiv N$ / Number of $C=N$ bonds
	0	3	384.4	$3 / 6 \cdot 1 = 0.50$
	1	5	640.7	$4 / 6 \cdot 2 = 0.33$
	2	7	896.9	$5 / 6 \cdot 3 = 0.28$

	3	9	1153.2	$6 / 6 \cdot 4 = 0.25$
	4	11	1409.4	$7 / 6 \cdot 5 = 0.23$

Ring Fragments: $(12 + 7n; n = 0, 1, 2, 3,...)$ multiples of 1,4-dicyanobenzene mass ($m/z = 128.1$)

Table S6 Ring fragments (oft CTF-1) observable in the mass spectra for the PTO samples and the specific nitrile-to-triazine ratio.

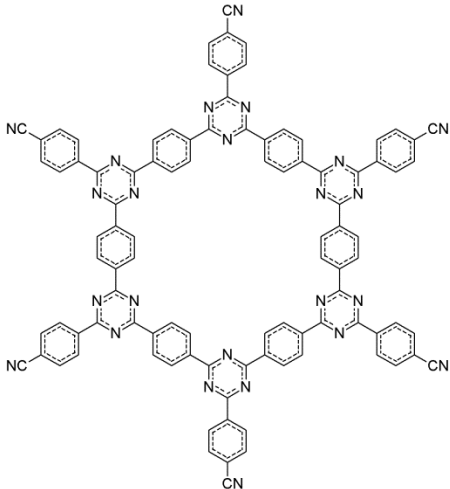
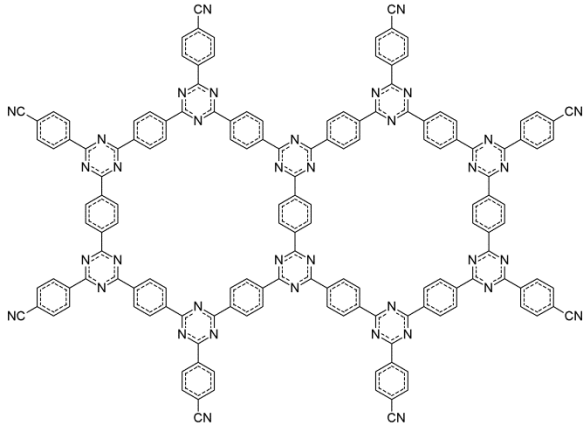
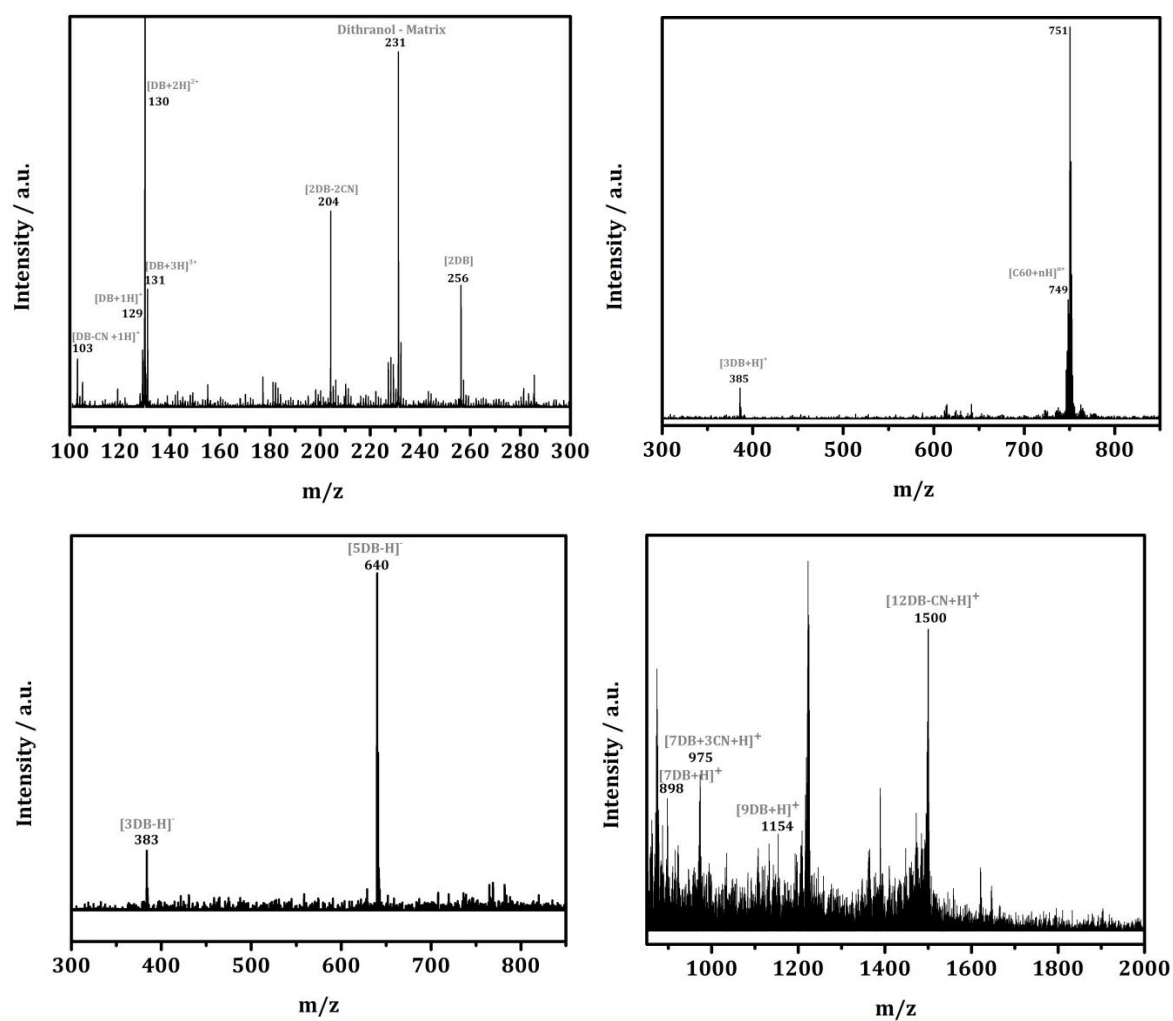
Chain Fragments	n	$(12+7n)$	m/z	Number of $C\equiv N$ / Number of $C=N$ bonds
	0	12	1537.6	$6 / 6 \cdot 6 = 0.17$
	1	19	2434.5	$8 / 6 \cdot 10 = 0.13$

Table S7 Nitrile-to-triazine ratios calculated from the IR signals (from signal intensities and integral, after background subtraction) of PTO-300-1 and PTOs-300 synthesized with higher zinc chloride dilution: PTO-300-2.5, PTO-300-10 and PTO-300-15 in comparison to the trimer.

Sample	Nitrile-to-triazine ratio (intensity)	Nitrile-to-triazine ratio (integral)
PTO-300-1	0.18 (0.18)	0.08 (0.09)
PTO-300-15	0.33 (0.32)	0.18 (0.16)
PTO-300-10	0.38 (0.46)	0.18 (0.23)
PTO-300-2.5	0.41	0.18
Trimer	0.51	0.29

Mass Spectra of PTO-300-1



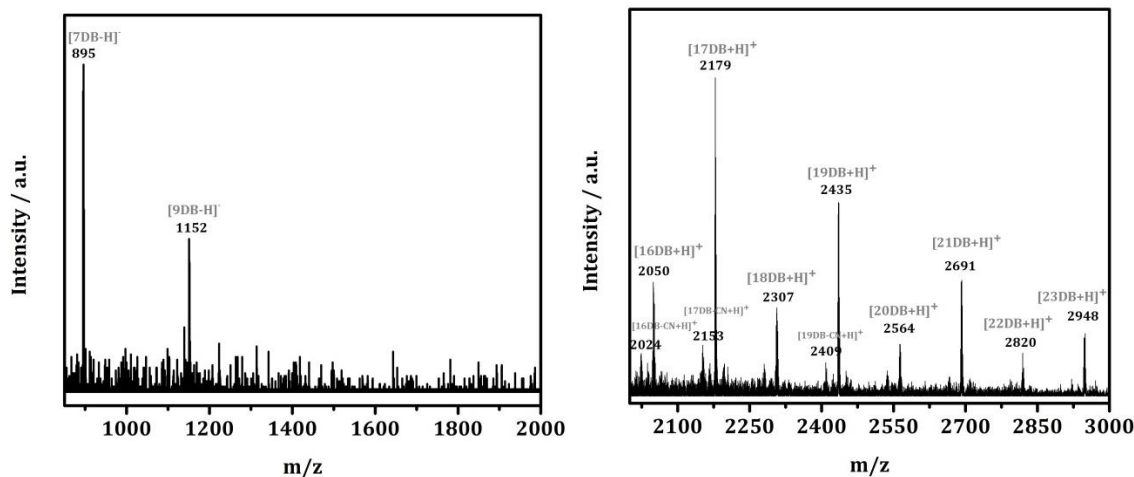
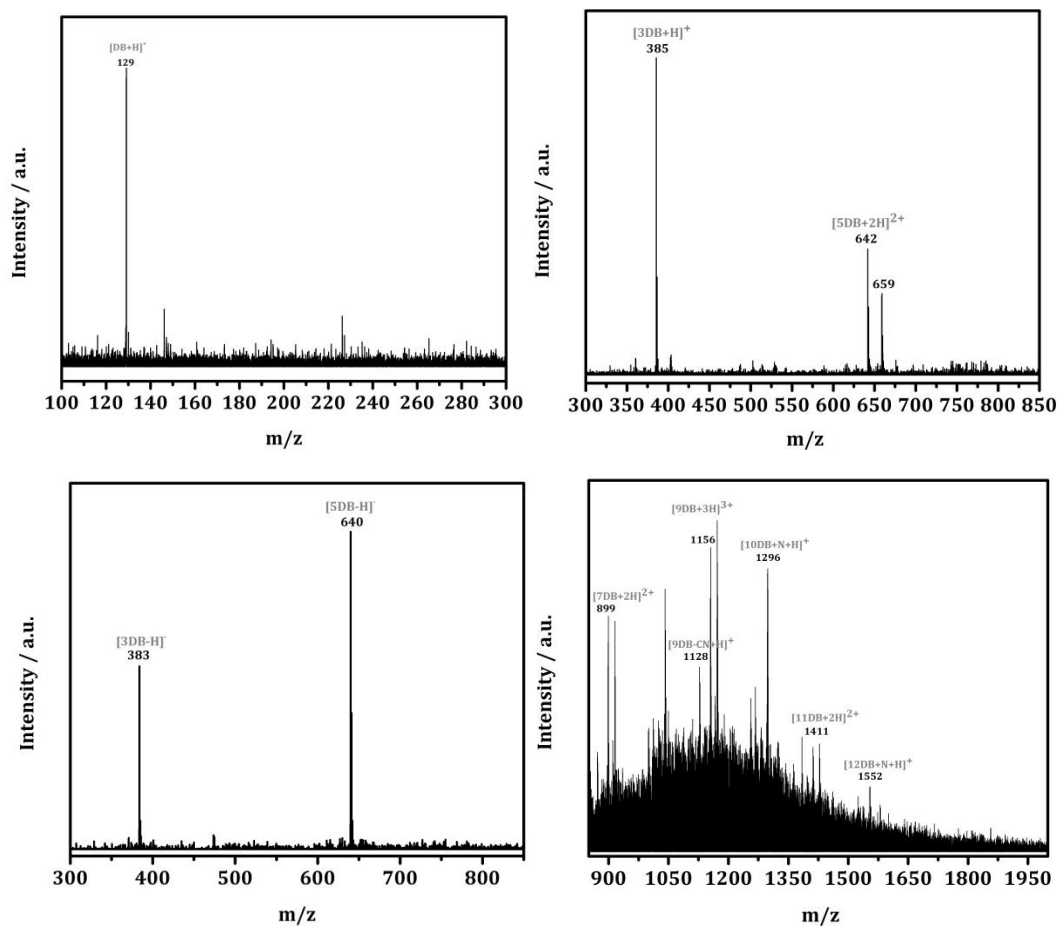


Fig. S7 Representative MALDI-TOF spectra of the PTO-300-1 sample, measured in the mass range > 100 and < 3000 (either in positive or negative mode, indicated with $+H^+$ or $-H^+$, respectively). DB represents the mass of the precursor 1,4-dicyanobenzene ($m/z = 128$). The signals at 230 and 750 correspond to the matrix.

Mass Spectra of PTO-300-15



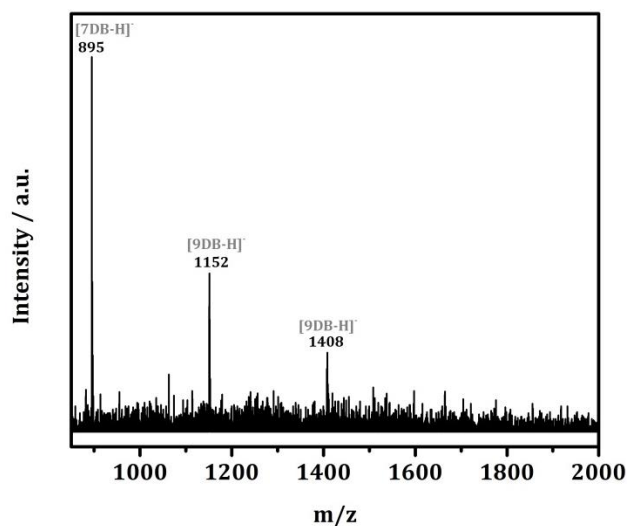
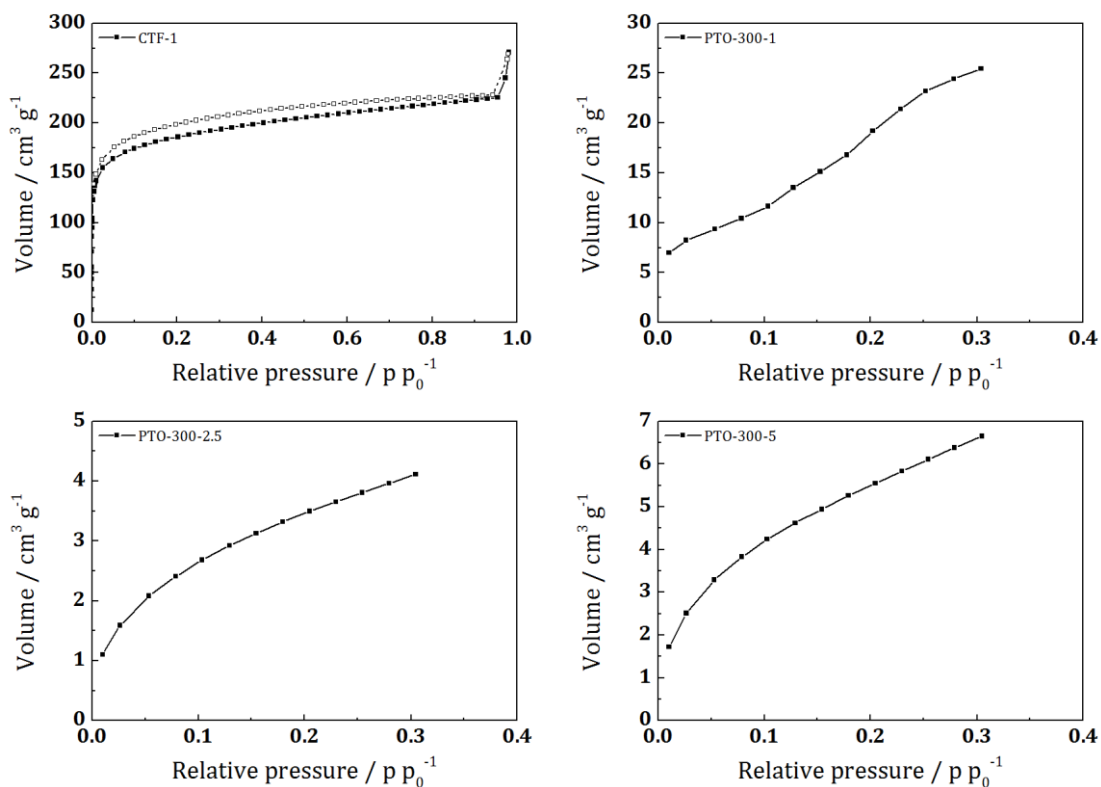


Fig. S8 Representative MALDI-TOF spectra of the PTO-300-15 sample, measured in the mass range > 100 and < 2000 (either in positive or negative mode, indicated with $+H^+$ or $-H^+$, respectively). DB represents the mass of the precursor 1,4-dicyanobenzene ($m/z = 128$). The signals at 230 correspond to the matrix.

Ar-Physisorption Measurements



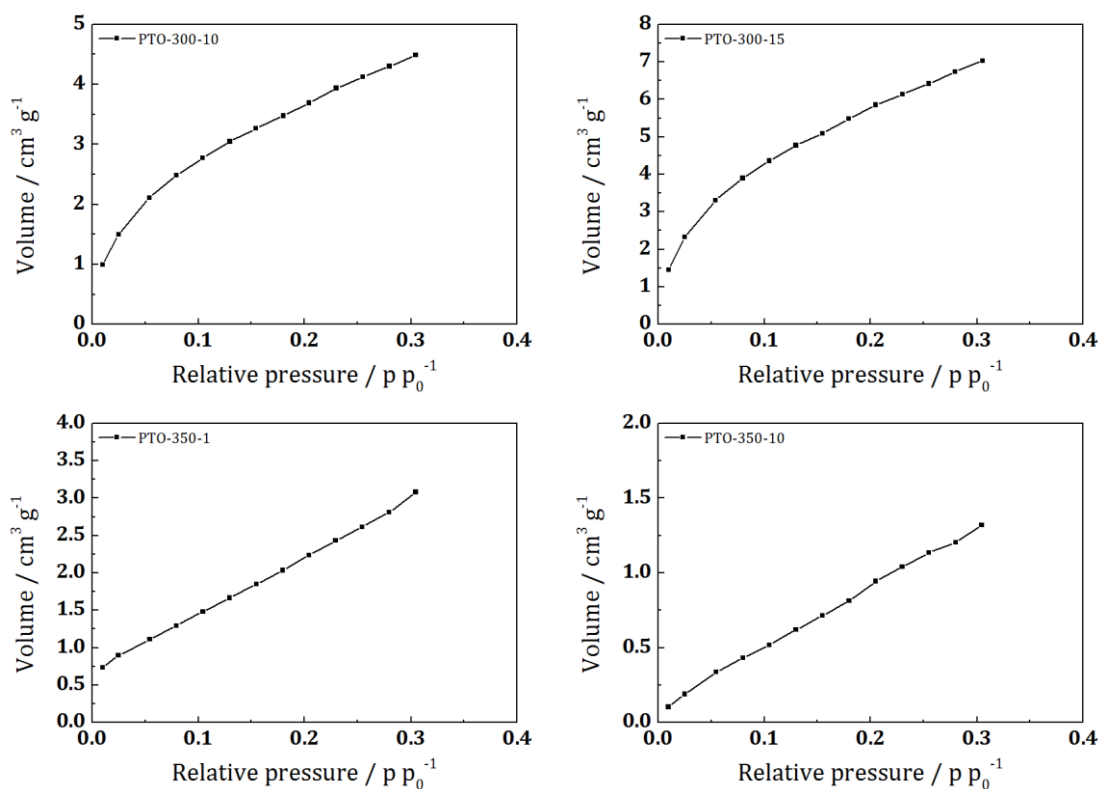
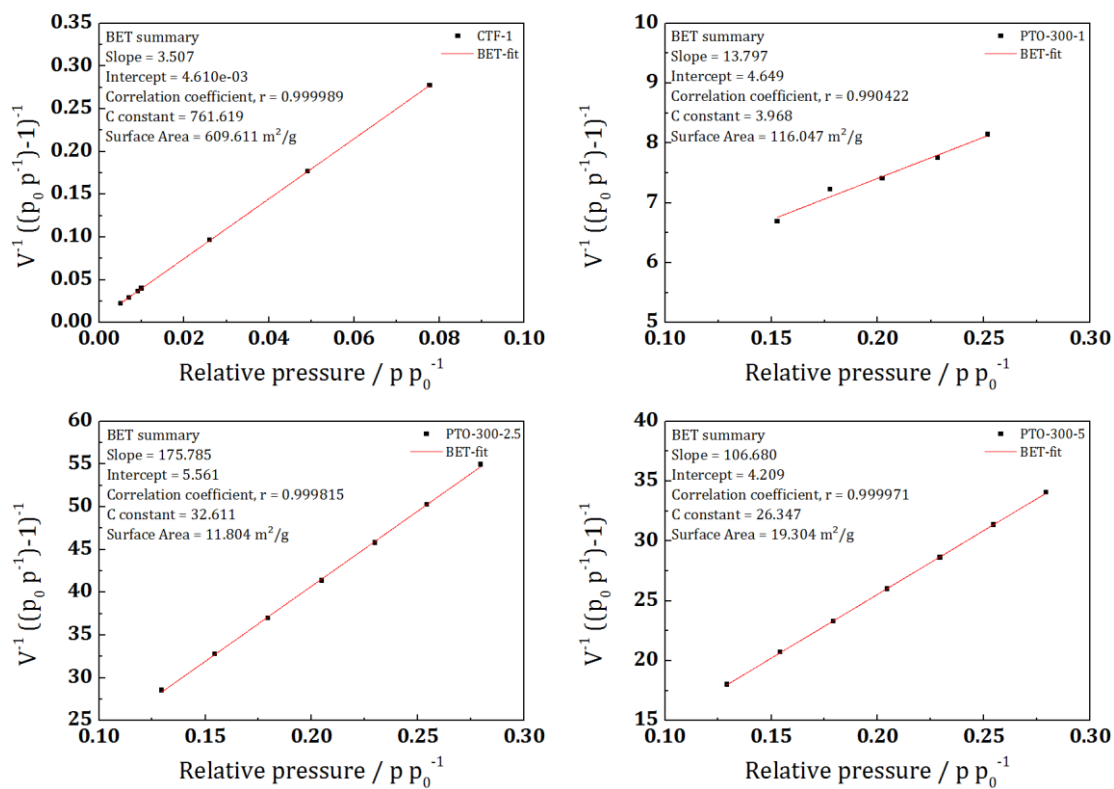


Fig. S9 Argon adsorption (filled squares) and desorption (empty squares) isotherm of CTF-1 and 13-point argon adsorption isotherms of PTO-300s and PTO-350s for BET calculations.



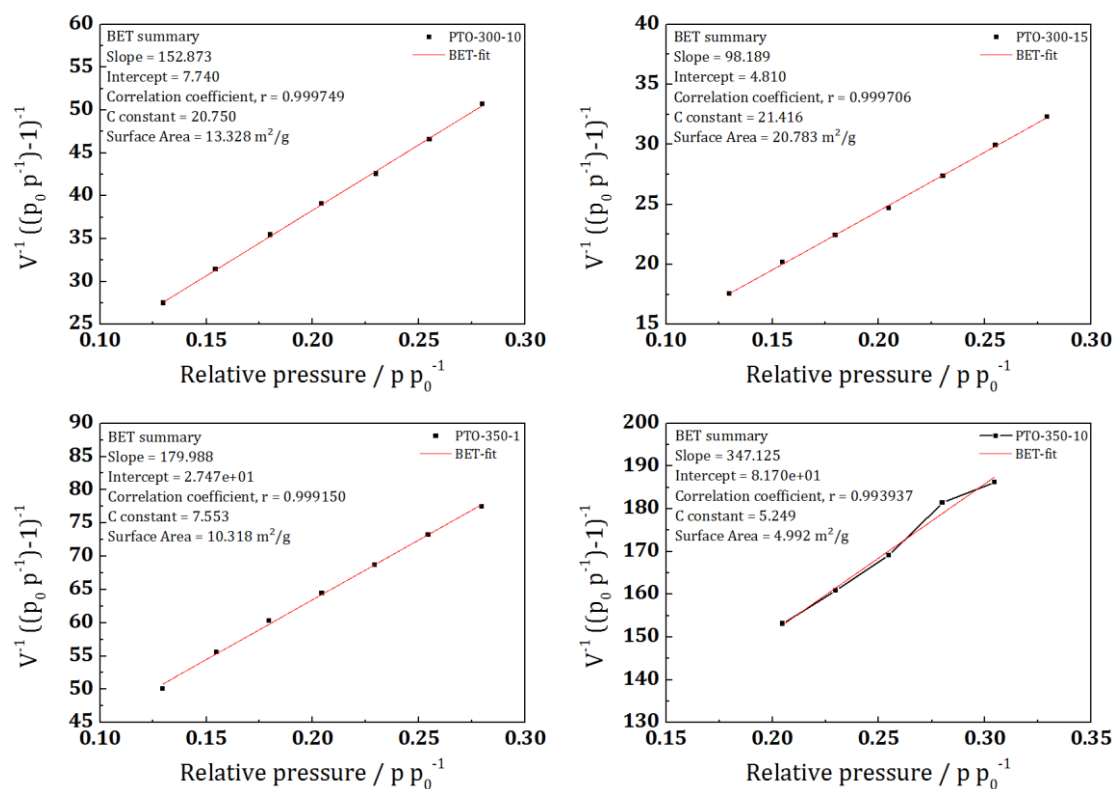


Fig. S10 BET-fits and BET calculation data of CTF-1, PTO-300s and PTO-350s. In accordance with the ISO recommendations multipoint BET tags equal or below the maximum in $V \cdot (1 - P/P_0)$ were chosen.

NMR Measurements

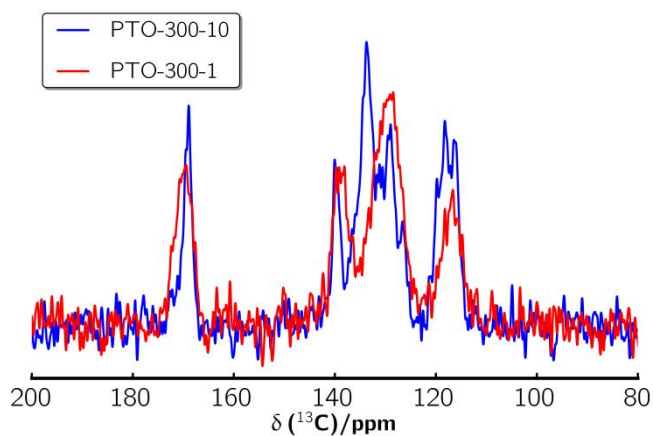


Fig. S11 ¹³C SP ssNMR spectra of PTO-300-10 and PTO-300-1 recorded with MAS using a rotational frequency of 20 kHz.

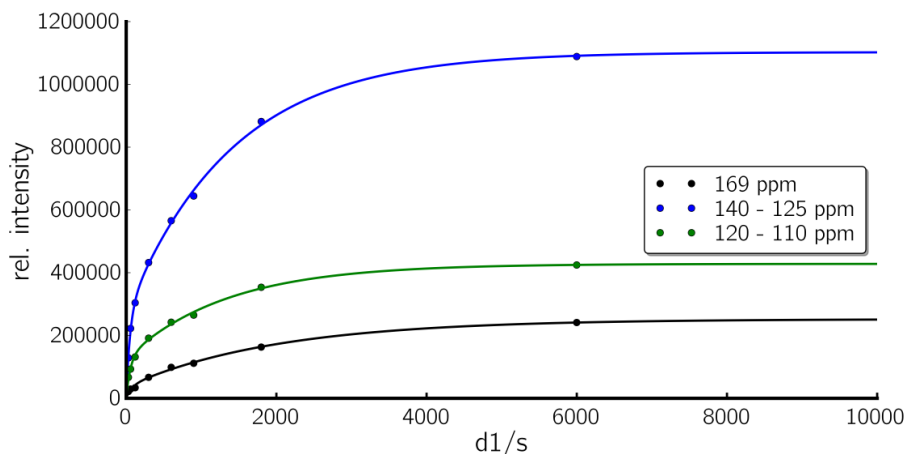


Fig. S12 Recycle delay plotted against signal intensity for ^{13}C SP ssNMR spectra of PTO-300-10 and fitted with the following biexponential function $I(x) = I_{0,1}(1 - \exp(-\frac{x}{T_{1,1}})) + I_{0,2}(1 - \exp(-\frac{x}{T_{1,2}}))$.

The values for I_0 and T_1 are presented in the following table.

	$I_{0,1}$	$T_{1,1} / \text{s}$	$I_{0,2}$	$T_{1,2} / \text{s}$
169 ppm	36716	742	215416	2013
140 – 125 ppm	268771	535	833953	1406
120 – 110 ppm	126903	570	301307	1334

The underestimation of the triazine signal due to the longer spin-lattice relaxation time was calculated from the ratio of the measured intensity at 6000 s to $I_{0,1} + I_{0,2}$ and gives about 5%. For the other signals this deviation is only about 1%.

Photocatalytic Experiments

Hydrogen Evolution Experiments

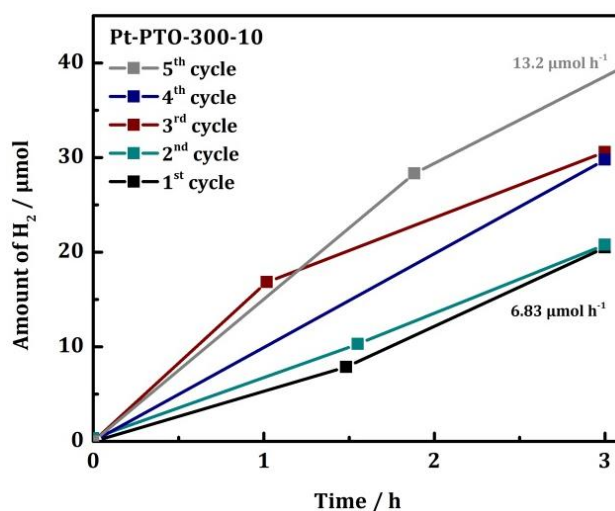


Fig. S13 Cyclic measurements with platinum-modified PTO-300-10 irradiated with simulated sunlight for three hours for each cycle. After each cycle the reactor was evacuated and purged with argon and irradiation was restarted.

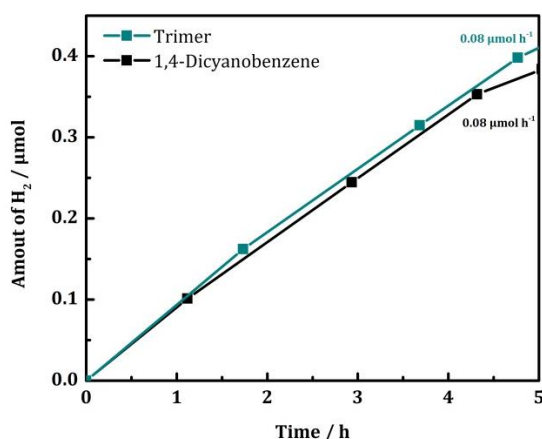


Fig. S14 Photocatalytic tests of the starting material 1,4-dicyanobenzene (black) and the trimer (cyan) using a buffered (pH 7, 0.5 M phosphate buffer) 10 vol% TEOA solution and platinum as co-catalyst during UV-Vis illumination (≥ 250 nm).

Table S8 Photocatalytic activity (with Pt as co-catalyst) *versus* the surface area.

Sample	BET SA [m ² g ⁻¹]	HER [μmol h ⁻¹]	HER [μmol h ⁻¹] / BET SA [m ² g ⁻¹]
PTO-300-1	116	1.45	0.01
PTO-300-2.5	12	6.91	0.58
PTO-300-5	19	3.36	0.18
PTO-300-10	13	9.00	0.69
PTO-300-15	21	9.40	0.48
CTF-1 as synthesized	610	0.02	0.00

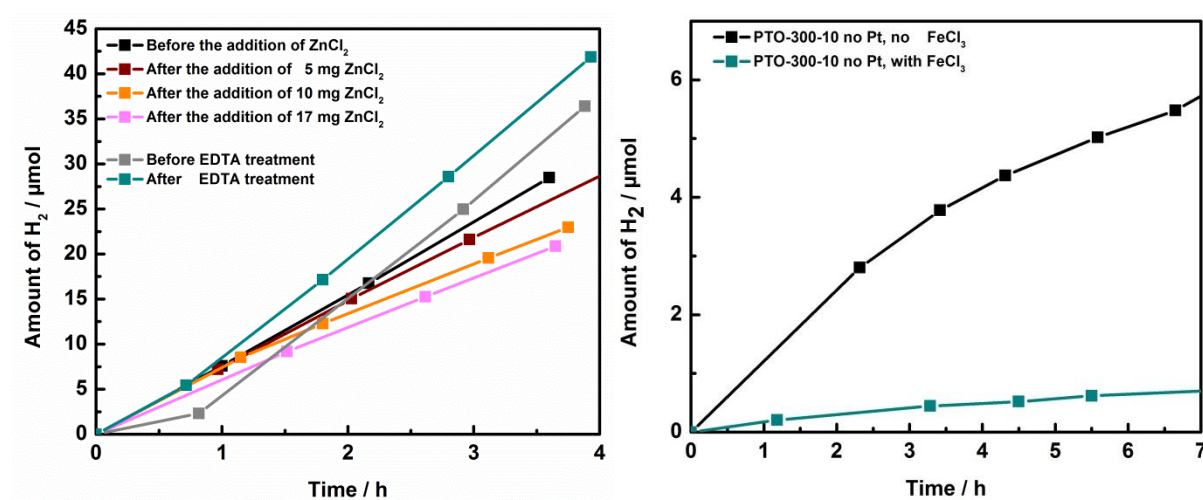


Fig. S15 Hydrogen evolution rates of Pt-PTO-300-10 before and after addition of several amounts (5, 10 or 17 mg) of ZnCl₂ and before and after stirring (for 2 days) / excessively washing the sample in EDTA (left). Hydrogen evolution rates (without the addition of H₂PtCl₆) of PTO-300-10 before and after stirring the sample in a FeCl₃ solution and an excessive washing procedure to achieve Fe³⁺ modification or, more accurately “poisoning” of the active site (likely the free electron pair at the nitrogen site of the nitrile group or the triazine) by coordination. However, the coordination mode is unclear, even if we can clearly

ascertain that iron is in the sample (see Table S9). The Fe^{3+} -treated sample showed a drastically decreased activity. The addition of platinum leads to an identical rate for both materials suggesting that not all active sites are poisoned by the Fe^{3+} or that platinum deposited on the Fe^{3+} site still promotes the electron transfer process.

Table S9 ICP data of the PTO-300-10 sample after/before EDTA treatment and Fe^{3+} poisoning.

Sample	Zn	Fe
PTO-300-10 before EDTA treatment	0.107	0.000
PTO-300-10 after EDTA treatment	0.079	0.000
PTO-300-10 after Fe^{3+} -poisoning	0.107	0.960

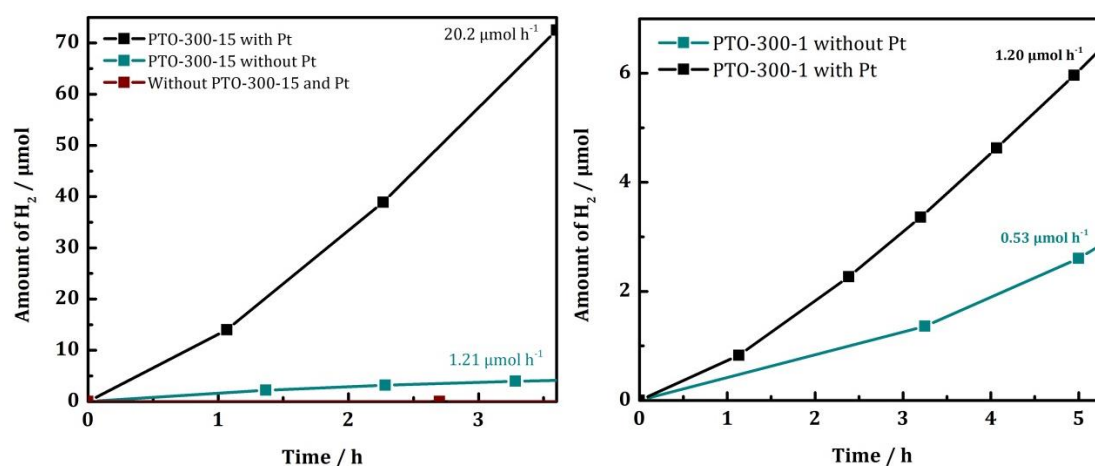


Fig. S16 Photocatalytic measurements (simulated sunlight) of dispersed PTO-300-15 (left) and PTO-300-1 (right) containing $6 \mu\text{L H}_2\text{PtCl}_6$ (black), in comparison to a photocatalysis run without the addition of platinum as co-catalyst (cyan). The red slope represents a control experiment showing the illuminated buffered TEoA solution without photocatalyst and platinum.

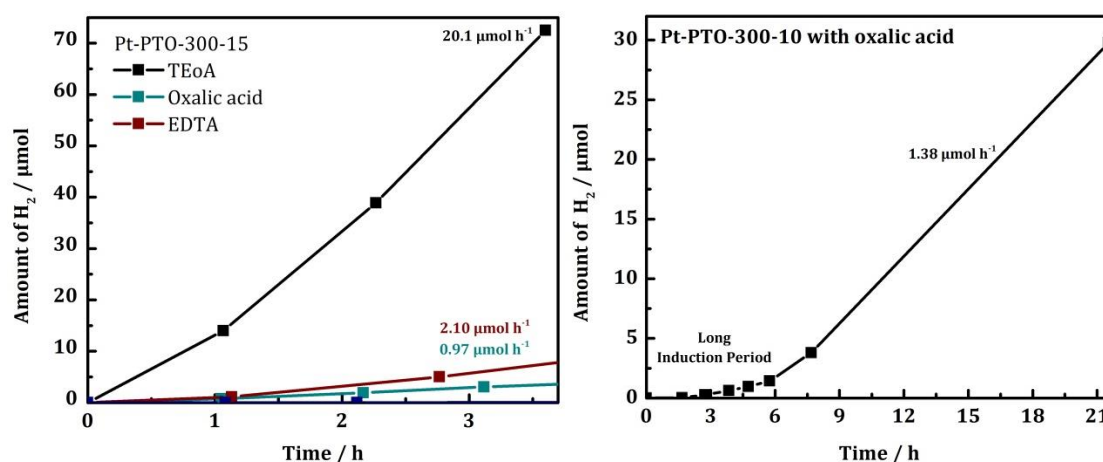


Fig. S17 Photocatalytic tests with Pt-PTO-300-15 (10 mL buffered - pH 7, 0.5 M phosphate buffer – electron donor solution, simulated sunlight, $6 \mu\text{L H}_2\text{PtCl}_6$) using different electron donors: TEoA (10 vol%;

black), oxalic acid (100 mg; cyan) and EDTA (10 vol%; red) (left). Stability test for more than 20 hours of Pt-PTO-300-10 using oxalic acid as electron donor (right).

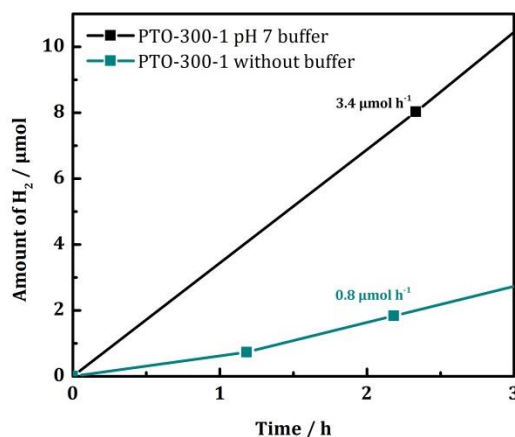


Fig. S18 Photocatalytic activity of Pt-PTO-300-1 dispersed in a phosphate buffered (pH 7, 0.5 M; black) compared to a non-buffered (cyan) 10 vol% TEoA solution illuminated with simulated sunlight.

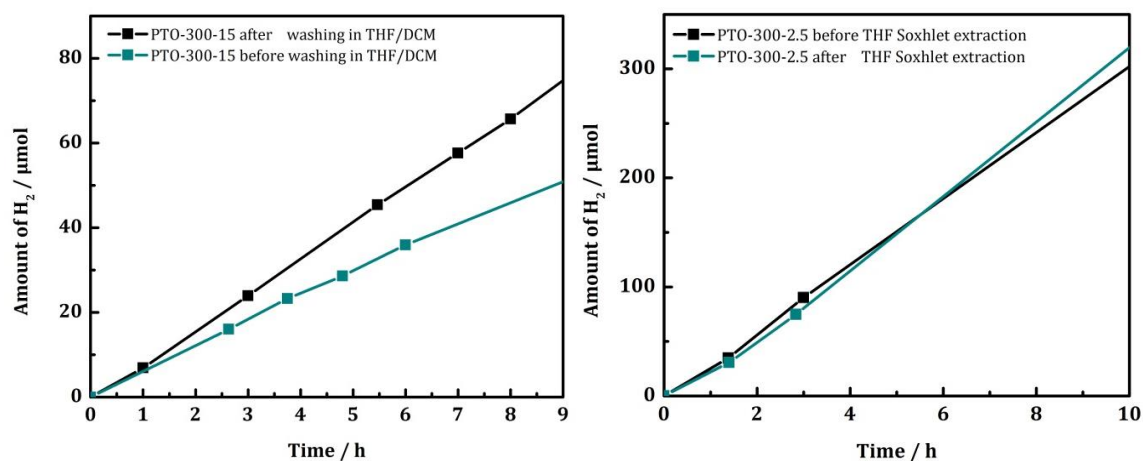


Fig. S19 Photocatalytic activity of Pt-PTO-300-15 before (cyan) and after (black) the first washing procedure with THF/DCM, showing that less active starting materials or rather small oligomers (such as trimers) are washed away (left). Photocatalytic activity of Pt-PTO-300-2.5 before (black) and after THF Soxhlet extraction (cyan) showing that the first washing procedure is sufficient to get rid of less active impurities (right).

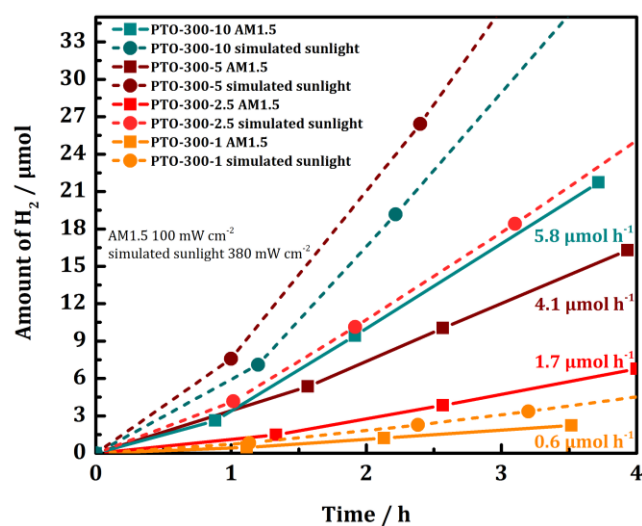


Fig. S20 Photocatalytic activity of four different PTO-300 samples under AM1.5 (100 mW cm⁻²) vs. simulated sunlight conditions (380 mW cm⁻²) (pH 7, 0.5 M phosphate buffer, 10 vol% TEOA solution, 2.2 wt% Pt).

Batch-to-Batch Variations

Table S10 Hydrogen evolution rates of several PTO-300 batches (Fig. S21). Colored values mark the “outlier” batches which were not used for the calculation of the “average” hydrogen evolution rate.

Sample	HER (several batches) / $\mu\text{mol h}^{-1}$ ^a
PTO-300-1	1.5, 1.5, 1.7
PTO-300-2.5	7.4, 8.0, 13.1, 15.6, 30.3
PTO-300-5	3.4 , 4.0 , 14.4, 15.8
PTO-300-10	8.3, 9.0, 9.9, 10.9
PTO-300-15	8.6, 8.7, 9.4, 11.6, 20.1

^aMeasurement error of 15%.

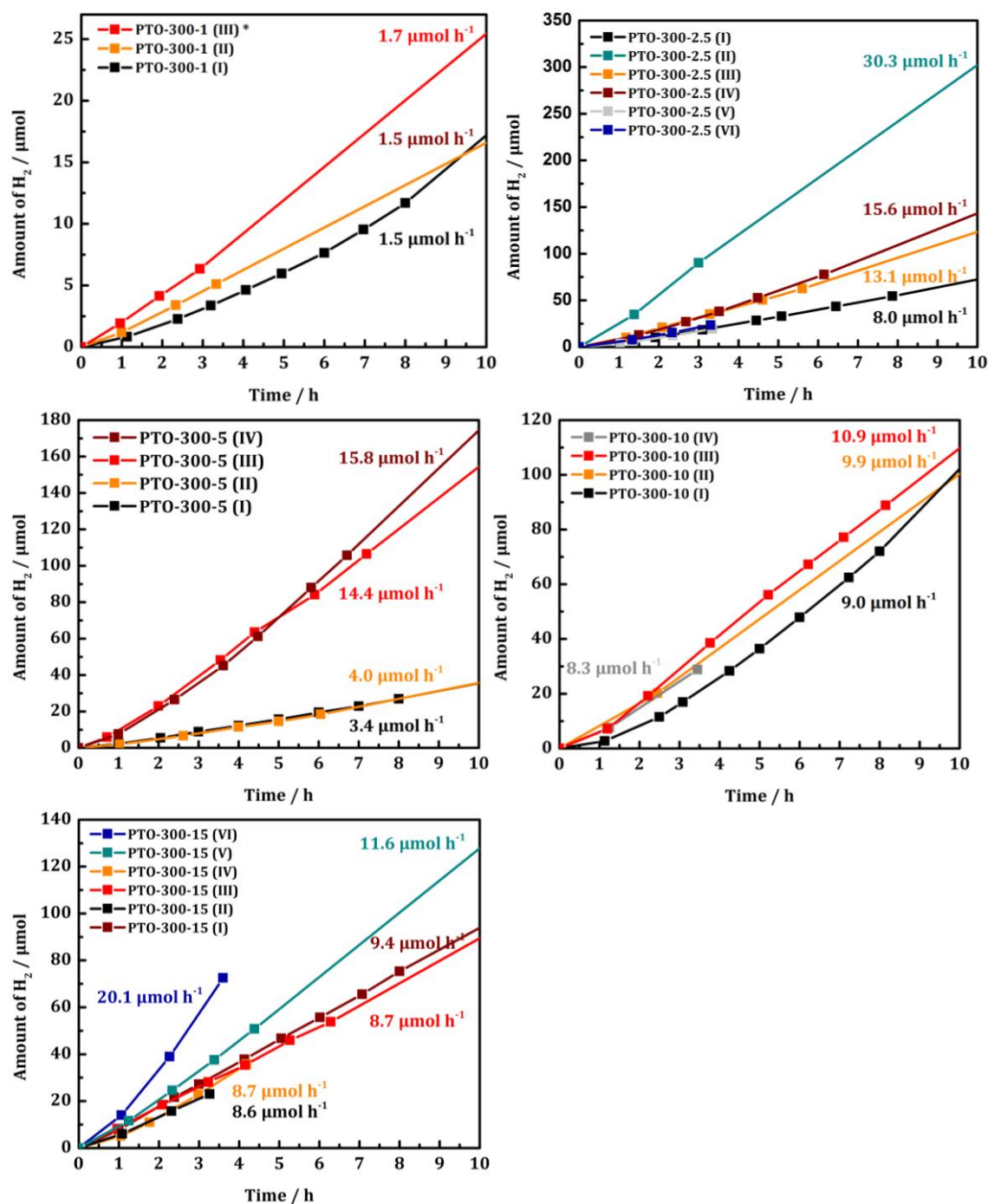


Fig. S21 Photocatalytic activity of various PTO-300 batches illuminated under simulated sunlight conditions (pH 7, 0.5 M phosphate buffer, 10 vol% TEOA solution, 2.2 wt% Pt) to illustrate batch-to-batch variations when synthesized in excess of ZnCl₂.

Characterization of the Photocatalyst after Photocatalysis

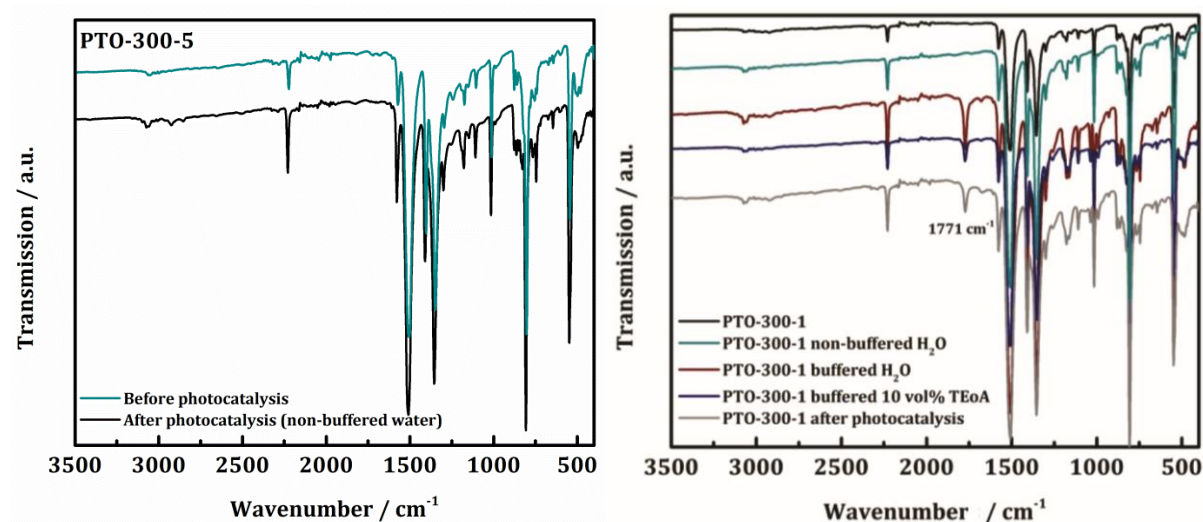


Fig. S22 IR spectroscopic characterization of the photocatalyst before (left: Pt-PTO-300-5; right: Pt-PTO-300-1) and after 24 hour of photocatalysis (left: in non-buffered water; right: in buffered water) as well as after each preparation step of the photocatalytic experiment: Stirring the photocatalyst in water or in pH 7 0.5 M phosphate buffer and after the addition of 10 vol% TEoA. A new band at 1771 cm⁻¹ appears due to the buffer. No changes caused by photodegradation.

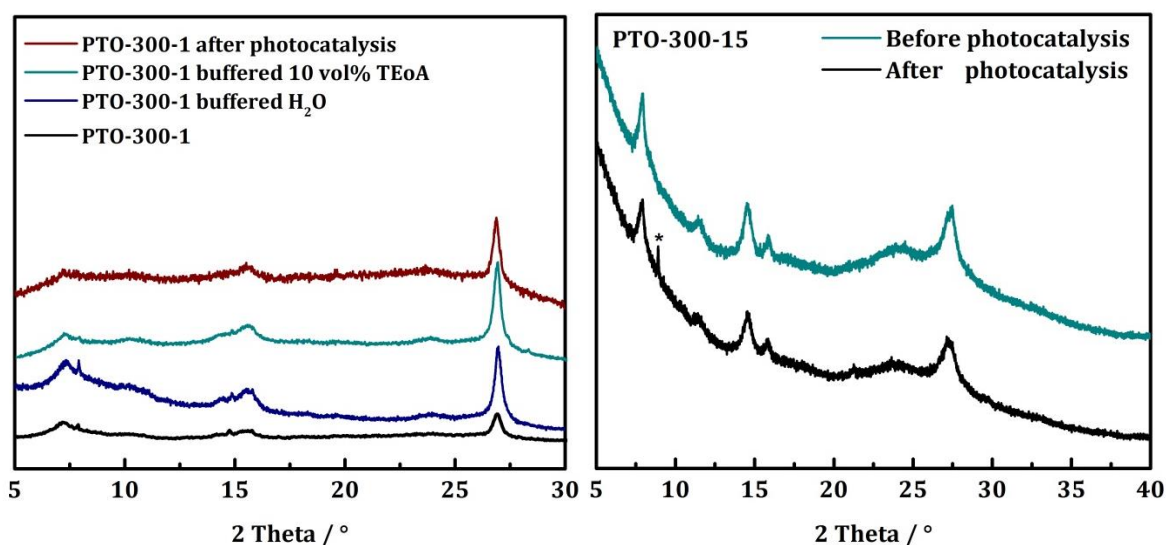


Fig. S23 PXRD of the photocatalyst PTO-300-1 (left) and PTO-300-15 (right) before and after 24 hour of photocatalysis in buffered water (left, Pt-PTO-300-1; right, Pt-PTO-300-15). In case of PTO-300-1, PXRD patterns are also shown after each preparation step of the photocatalytic experiment: Stirring the photocatalyst in pH 7 0.5 M phosphate buffer and after the addition of 10 vol% TEoA. The sharp reflection marked with an asterisk is an artefact due to the sample holder.

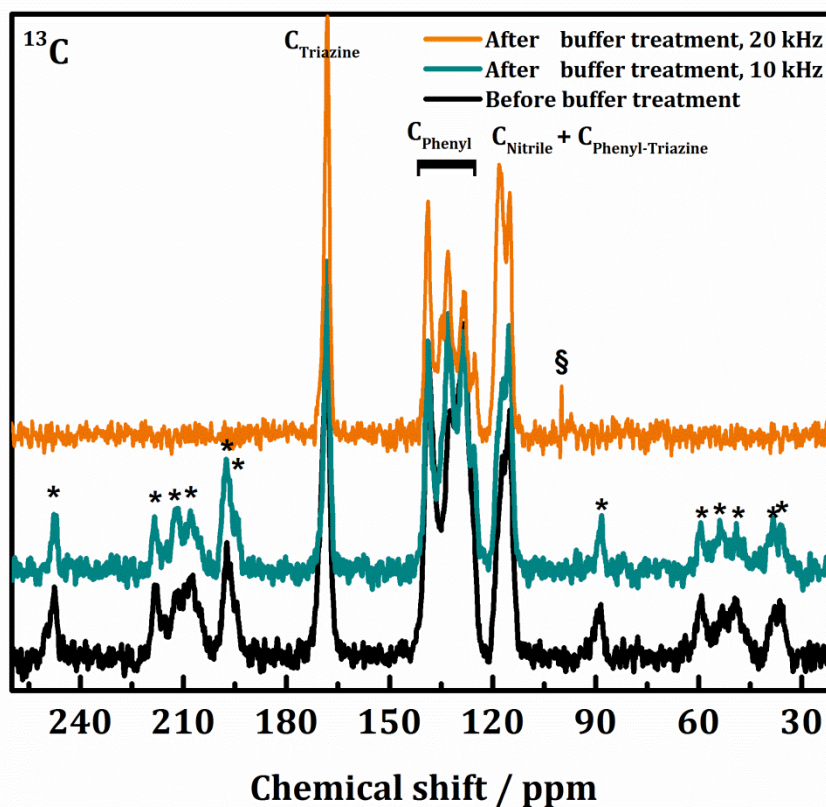


Fig. S24 Solid state NMR ^{13}C spectra (contact time 5 ms) of PTO-300-15 before (spinning speed 10 kHz) and after (spinning speed 10 and 20 kHz) stirring the photocatalyst three days in buffered water (pH 7, 0.5 M phosphate buffer). Bands marked with an asterisk are rotational side bands. The sharp peak marked with “\$” is an artefact. No additional carbon signals are detected after buffer treatment which makes hydrolysis of the nitrile groups unlikely.

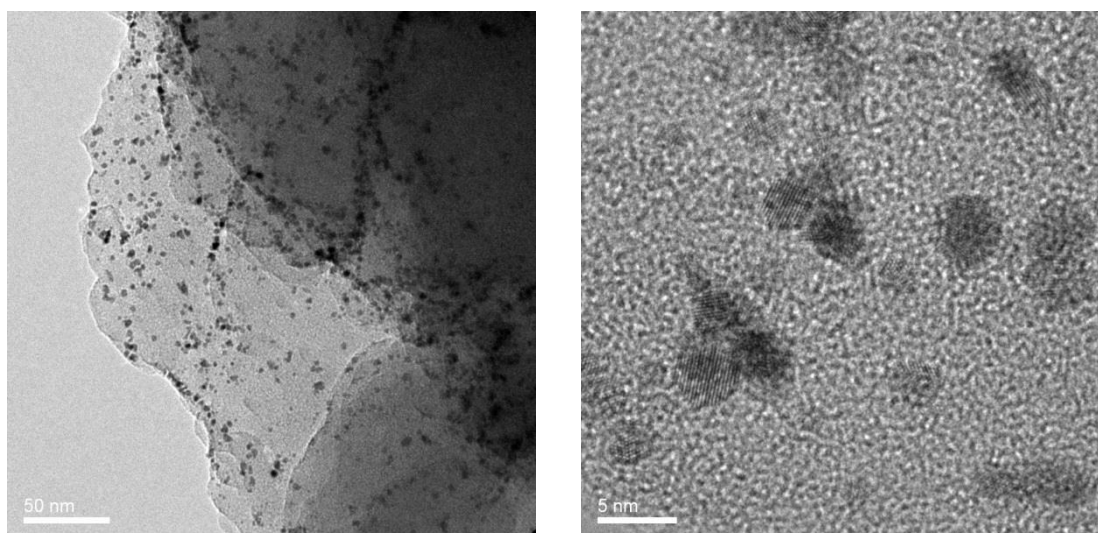


Fig. S25 TEM images of the Pt-modified PTO-300-1 sample after photocatalysis. Pt-nanoparticles around 4 nm of average size have been formed on the sample surface after photo-reduction of H_2PtCl_6 .

TEM Characterization

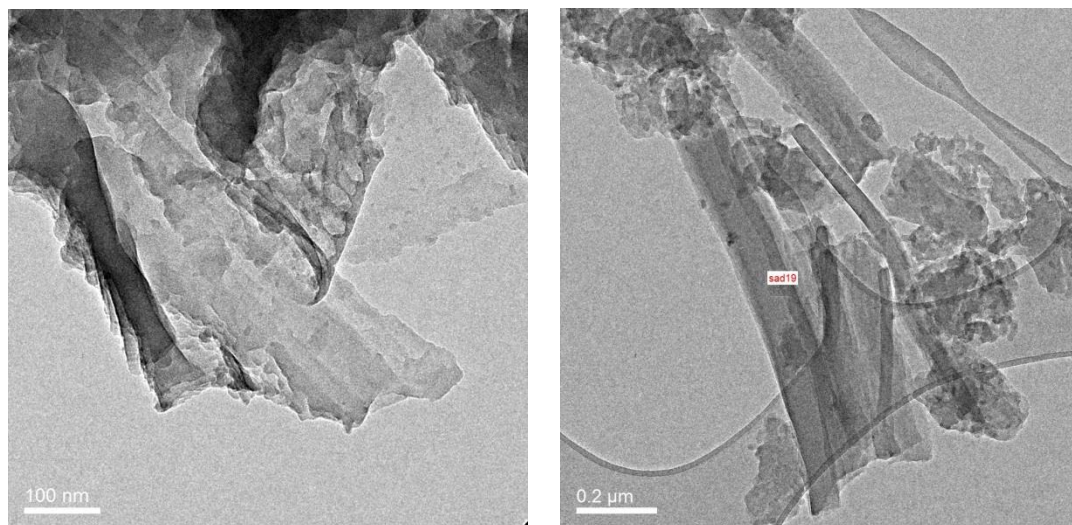


Fig. S26 TEM image of PTO-300-1 showing a layered-like material (left). TEM image of PTO-300-10 showing mixed phases of clusters and either fibers or furled layers (right).

References

- S1 P. Kuhn, M. Antonietti and A. Thomas, *Angew. Chem. Int. Ed.*, 2008, **47**, 3450.
- S2 H. Tanaka, K. Shizu, H. Nakanotani and C. Adachi, *C. Chem. Mater.*, 2013, **25**, 3766.
- S3 X. Wang, K. Maeda, A. Thomas, K. Takanabe, G. Xin, J. M. Carlsson, K. Domen and M. Antonietti, *Nat. Mater.*, 2009, **8**, 76.
- S4 K. Schwinghammer, B. Tuffy, M. B. Mesch, E. Wirnhier, C. Martineau, F. Taulelle, W. Schnick, J. Senker and B. V. Lotsch, *Angew. Chem. Int. Ed.*, 2013, **52**, 2435.
- S5 L. Stegbauer, K. Schwinghammer and B. V. Lotsch, *Chem. Sci.*, 2014, **5**, 2789.
- S6 K. Schwinghammer, M. B. Mesch, V. Duppel, C. Ziegler, J. Senker and B. V. Lotsch, *J. Am. Chem. Soc.*, 2014, **136**, 1730.
- S7 S. Ren, M. J. Bojdys, R. Dawson, A. Laybourn, Y. Z. Khimyak, D. J. Adams, A. I. Cooper, *Adv. Mater.*, 2012, **24**, 2357.